Biochimica et Biophysica Acta 1854 (2015) 1458–1465

Contents lists available at ScienceDirect

Biochimica et Biophysica Acta

journal homepage: www.elsevier.com/locate/bbapap

Multiple disulfide bridges modulate conformational stability and flexibility in hyperthermophilic archaeal purine nucleoside phosphorylase

Maria Libera Bagarolo [a], Marina Porcelli [a], Elisa Martino [a], Georges Feller [b], Giovanna Cacciapuoti [a,*]

[a] Dipartimento di Biochimica, Biofisica e Patologia Generale, Seconda Università di Napoli, Via Costantinopoli 16, 80138 Naples, Italy
[b] Laboratory of Biochemistry, Centre for Protein Engineering, University of Liège, Liège B-4000, Belgium

ARTICLE INFO

Article history:
Received 25 March 2015
Received in revised form 27 May 2015
Accepted 23 June 2015
Available online 24 June 2015

Keywords:
5′-Deoxy-5′-methylthioadenosine phosphorylase II from *S. solfataricus*
Hyperthermophilic enzymes
Protein thermostability
Disulfide bridges
Differential scanning calorimetry
Limited proteolysis

ABSTRACT

5′-Deoxy-5′-methylthioadenosine phosphorylase from *Sulfolobus solfataricus* is a hexameric hyperthermophilic protein containing in each subunit two pairs of disulfide bridges, a CXC motif, and one free cysteine. The contribution of each disulfide bridge to the protein conformational stability and flexibility has been assessed by comparing the thermal unfolding and the limited proteolysis of the *wild-type* enzyme and its variants obtained by site-directed mutagenesis of the seven cysteine residues. All variants catalyzed efficiently MTA cleavage with specific activity similar to the *wild-type* enzyme. The elimination of all cysteine residues caused a substantial decrease of ΔH_{cal} (850 kcal/mol) and T_{max} (39 °C) with respect to the *wild-type* indicating that all cysteine pairs and especially the CXC motif significantly contribute to the enzyme thermal stability. Disulfide bond Cys200–Cys262 and the CXC motif weakly affected protein flexibility while the elimination of the disulfide bond Cys138–Cys205 lead to an increased protease susceptibility. Experimental evidence from limited proteolysis, differential scanning calorimetry, and sodium dodecyl sulfate-polyacrylamide gel electrophoresis under reducing and nonreducing conditions also allowed to propose a stabilizing role for the free Cys164.

© 2015 Elsevier B.V. All rights reserved.

1. Introduction

Hypertermophilic organisms grow optimally at temperature near or above 100 °C. Therefore, their proteins must remain folded and functional at these high temperatures, keeping the required stability and structural flexibility. Understanding the mechanisms of this enhanced thermostability in such proteins has become a fundamental goal in the field of protein biochemistry. In fact, not only these proteins provided unique insights into the rules governing protein folding, stability and structural flexibility, but their peculiar structure–function properties are potentially significant for developing biotechnological applications through protein engineering. Studying different mechanisms by which proteins increase or decrease stability sheds light on the fundamentals of protein thermodynamics and can contribute to design new enzymes with desired stability [1–5]. The crystal structures of many hyperthermophilic proteins have been determined, and several factors responsible for their extreme thermostability have been proposed [6–10], including increases in the number of ion pairs and hydrogen bonds, core hydrophobicity and packing density, as well as the oligomerization of several subunits, and an entropic effect due to the relatively shorter surface loops and polypeptide chains. It has been recently reported that some proteins from hyperthermophiles are characterized by remarkably slow unfolding rates and it has been suggested that a kinetic barrier towards unfolding may be a common strategy used by many proteins to withstand extreme conditions [11,12]. However, although many theoretical and experimental studies have been carried out in the past, no general mechanism for increased thermostability was established to date. Proteins attain stability through a combination of many factors that contribute, in different proteins, to various extents.

In spite of the classical view that stabilizing disulfide bonds are rare in intracellular proteins from well known organisms due to the reducing chemical environment inside the cells [13], recent computational, structural and biochemical studies have pointed out the critical role of these covalent links in the structural stabilization of intracellular proteins of some hyperthermophilic *Archaea* and *Bacteria*[14–19]. The abundance of disulfides observed across hyperthermophilic organisms also stimulated research into the identification of the biochemical mechanisms related to disulfide maintenance. It has been demonstrated that specific

Abbreviations: SsMTAPII, 5′-deoxy-5′-methylthioadenosine phosphorylase II from *Sulfolobus solfataricus*; PNP, purine nucleoside phosphorylase; AdoMet, S-adenosylmethionine; MTA, 5′-deoxy-5′-methylthioadenosine; PDI, protein-disulfide isomerase, DSC, differential scanning calorimetry; SDS-PAGE, sodium dodecyl sulfate-polyacrylamide gel electrophoresis; CD, circular dichroism; [θ], molar ellipticity per mean residue; GdmCl, guanidinium chloride; PIPES buffer, piperazine-N,N′-bis(ethanesulfonic acid); NDSB, 3-(1-Pyridinio)-1-propanesulfonate; MOPS, 3-(N-morpholino) propanesulfonic acid.

* Corresponding author.
E-mail address: giovanna.cacciapuoti@unina2.it (G. Cacciapuoti).

http://dx.doi.org/10.1016/j.bbapap.2015.06.010
1570-9639/© 2015 Elsevier B.V. All rights reserved.

protein-disulfide oxidoreductases [20], structurally and functionally related to protein-disulfide isomerase (PDI) [21], play a key role in intracellular disulfide-shuffling in hyperthermophilic proteins.

Purine nucleoside phosphorylases (PNPs) are ubiquitous enzymes of purine metabolism that function in the purine salvage pathway of the cells [22,23]. All archaeal PNPs so far characterized, are extremely thermophilic and thermostable proteins with temperature optima and melting temperature above 100 °C and are stabilized by disulfide bridges [15,18,19,24].

5′-Deoxy-5′-methylthioadenosine phosphorylase II from the archaeon *Sulfolobus solfataricus* (SsMTAPII), a member of the archaeal family PNPs, is a hyperthermophilic enzyme that has been fully characterized by its physicochemical, kinetic and structural properties [24]. The presence in SsMTAPII of multiple intrasubunit disulfide bonds offers a good opportunity to elucidate the contribution of these covalent links in preserving the native conformation of a protein at extreme environmental temperature.

SsMTAPII is a homohexamer characterized by extremely high affinity towards 5′-deoxy-5′-methylthioadenosine (MTA), a sulfur-containing nucleoside generated from S-adenosylmethionine (AdoMet) mainly through polyamine biosynthesis [25]. SsMTAPII also accepts adenosine as substrate [24].

SsMTAPII is a tightly packed protein of 180 kDa, as shown by its tridimensional structure solved to 1.45 Å resolution (PDB entry code 2A8Y) [26]. The hexameric structure of SsMTAPII is a dimer-of-trimers with one active site per monomer. The oligomeric assembly of the trimer and the monomer topology of SsMTAPII are almost identical to trimeric human 5′-deoxy-5′-methylthioadenosine phosphorylase [23]. Therefore, SsMTAPII can be regarded as the first reported hexamer in the trimeric class of PNP from *Archaea*. SsMTAPII contains seven cysteine residues per monomer. Four cysteine residues form two pairs of intrasubunit disulfide bridges, Cys138–Cys205 and Cys200–Cys262, near the C-terminus of the protein. The seventh cysteine, Cys164, is free. Each subunit contains in its C-terminal region a CXC motif (i.e. a couple of cysteine residues separated by one amino acid X) as a typical feature. This motif is very close to the two pairs of disulfide bridges that are separated at a distance of 8.5 Å from the centers of disulfide bonds. By enzymatic activity measurements it has been demonstrated that the substitution of these two cysteine residues (C259 and C261) with serine results in a significant decrease of thermal stability parameters of SsMTAPII [24] and that this unusual CXC disulfide is necessary to obtain a complete unfolding reversibility of the protein [27]. The biochemical characterization of SsMTAPII has highlighted features of exceptional thermostability, with an optimum temperature for activity of 120 °C, an apparent melting temperature (Tm) of 112 °C and a notably high stability towards irreversible thermal inactivation processes. Moreover, SsMTAPII possess a remarkable resistance to sodium dodecyl sulfate (SDS), proteolytic cleavage, and guanidinium chloride (GdmCl)-induced unfolding [24].

In this study, the quantitative contribution of disulfide bonds to thermal stability of SsMTAPII was assessed by a comparative kinetic and calorimetric analysis of the *wild-type* enzyme and of its mutants obtained by site-directed mutagenesis of the seven cysteine residues in the monomer. Furthermore, using limited proteolysis we were able to probe the structural and dynamic differences among SsMTAPII and its cysteine-laking mutants, therefore obtaining relevant information on the involvement of disulfide bridges in the enzyme conformational flexibility.

2. Experimental procedures

2.1. Bacterial strains, plasmid, enzymes and chemicals

E*scherichia coli* strain BL21 (λDE3) was purchased from Novagen (Darmstadt, Germany). *S. solfataricus* chromosomal DNA was kindly provided by Prof. A. Gambacorta (Institute of Biomolecular Chemistry ICB-CNR. Naples). Plasmid pET-22b(+) and the NucleoSpin Plasmid kit for plasmid DNA preparation were obtained from Genenco (Duren, Germany). Specifically synthesized oligodeoxyribonucleotides were obtained from MWG-Biotech (Ebersberg, Germany). Restriction endonucleases and DNA-modifying enzymes were obtained from Takara Bio, Inc. (Otsu, Shiga, Japan). *Pfu* DNA polymerase was purchased from Stratagene (La Jolla, CA, USA).

MTA was prepared from AdoMet [28]. Nucleosides, purine bases and proteinase K were obtained from Sigma (St. Louis, MO, USA). Standard proteins were supplied by Applied Biological Materials Inc. (Richmond, BC, Canada). PIPES piperazine-N,N′-bis(2-ethanesulfonic acid) was from Applichem (Darmstadt, Germany). 3-(1-Pyridinio)-1-propanesulfonate (NDSB), 3-(N-morpholino) propanesulfonic acid (MOPS) and proteinase K were from Sigma. All buffers and solutions were prepared with ultra-high quality water. All reagents were of the purest commercial grade.

2.2. Site-directed mutagenesis, expression and purification of SsMTAPII mutants

The sequence of *SsMTAPII* gene (GenBank™ accession number AE006641) from *S. solfataricus* was previously inserted in the *Nde1-EcoR1* cloning site of the pET-22b(+) expression vector [24]. Site-directed mutants were prepared following the QuickChange site-directed mutagenesis protocol (Stratagene, La Jolla, CA) using the construct pET-SsMTAPII as a template. Primers for site-directed mutagenesis were designed according to the instructions for the Quick-Change kit. SsMTAPII mutants Cys262Ser (*mut1*) and Cys259Ser:Cys261Ser (*mut2*) were obtained by mutating Cys-262 and Cys259-Cys261, respectively, in the *wild-type* SsMTAPII gene. The mutants Cys259Ser:Cys261Ser:Cys262Ser (*mut3*),Cys259Ser:Cys261Ser:Cys262Ser:Cys200Ser:Cys205Ser (*mut4*),Cys259Ser:Cys261Ser:Cys262Ser:Cys200Ser:Cys205Ser:Cys138Ser (*mut5*), and Cys259Ser:Cys261Ser:Cys262Ser:Cys200Ser:Cys205Ser:Cys138Ser:Cys164Ser (*mut6*), were generated by mutating, in sequence, Cys259-Cys261-Cys262, Cys200-Cys205, Cys138, and Cys164 in the *wild-type* SsMTAPII gene. The primers used are the following: 5′-GGTCGTGTTCCTGTAGCAACAGTCTGAAGACAG-3′ sense and 5′-CTGTCTTCAGACTGTTGCTACAGGAACACGACC-3′ antisense (*mut1)*; 5′-CAGAAGAGGGGTCGAGTTCCAGTTGCAACAGTC-3′ sense and 5′-GACTGTTGCAACTGGAACTCGACCCCTCTTCTG-3′ antisense (*mut2)*;5′-GAGTTCCAGTAGCAACAGTCTGAAGACAG-3′ sense and 5′-GTTGCTACTGGAACTCGACCCCTC-3′ antisense (*mut3)*; 5′-GAGTGAGGCACAAATGAGTTATGCCAC-3′ sense and 5′-CTCATTTGTGCCTCACTCGCAAGATTAAC-3′ antisense (*mut4*); 5′-GATCCATTTAGTAATAGCTTAAGGAAATTGGC-3′ sense and 5′-GCTATTACTAAATGGATCAGCCATTGAGAC-3′ antisense (*mut5*); 5′-ACCTATATAAGTATTGAGGGTCCTAGGTTTTCTAC-3′ sense and 5′-CTCAATACTTATATAGGTACCACTTTCATGCGTC-3′ antisense (*mut6*). Mutations were confirmed by DNA sequencing.

The expression of SsMTAPII mutants in *E. coli* BL21(λDE3) cells and the purification of the recombinant proteins were carried out following the procedures previously described for the *wild-type* enzyme [24]. Manipulations of DNA and E. *coli* were carried out using standard protocols [29]. Proteins were analyzed by sodium dodecyl sulfate–polyacrylamide gel electrophoresis (SDS-PAGE) as described by Weber et al. [30] and quantified with the Bradford assay [31] or estimated spectrophotometrically using the theoretical sequence-based coefficient of 33,265 M^{-1} cm^{-1} calculated at 280 nm for the hexameric protein [32].

2.3. Enzyme preparation and assay

MTA phosphorylase activity of SsMTAPII and its mutants was determined by measuring the formation of adenine from MTA. Unless otherwise stated, the standard incubation mixture contained the following: 20 μmol potassium phosphate buffer, pH 7.4, 400 nmol of MTA and

the enzyme protein in a final volume of 200 μL. The incubation was performed in sealed glass vials for 5 min at 70 °C. The vials were rapidly cooled in ice, and the reaction was stopped by the addition of 50 μL of 3% (v/v) trifluoroacetic acid. Control experiments in the absence of the enzyme were performed in order to correct for spontaneous nucleoside hydrolysis. The formation of adenine base was measured by HPLC using a Beckman system Gold apparatus and a 5 μm Dionex C-18 column (4.6 × 250 mm). The elution was carried out with a mixture of 20:80 (v/v) 95% methanol and 0.1% trifluoroacetic acid in water at a flow rate of 1 mL min^{-1}. The amount of purine base formed was determined by measuring the percentage of the absorbance integrated peak area of purine base formed with respect to the total (nucleoside + purine base) absorbance integrated peak areas. In all of the kinetic and purification studies the amounts of the protein was adjusted so that no more than 15% of the substrate was converted to product and the reaction rate was strictly linear as a function of time and protein concentration. All enzyme reactions were performed in triplicate. Values given are the average from at least three experiments with standard errors.

2.4. Temperature dependence and thermostability of activity

The temperature dependence of SsMTAPII and its mutants was studied by measuring the enzymatic activity in the temperature range from 40 °C to 120 °C. Enzyme thermostability was investigated by carrying out short time kinetics of thermal denaturation. The proteins were preincubated for 5 min in sealed glass vials at temperature between 50 °C and 120 °C in an oil bath. Residual activity was determined in standard conditions by the addition of aliquots from each preincubated sample.

2.5. Differential scanning calorimetry

Measurements were performed using a MicroCal VP-DSC instrument at a scan rate of 90 K h^{-1} and under ~25 psi positive cell pressure. Samples were dialyzed overnight against 30 mM MOPS, pH 7.0. After dialysis, both the sample and the reference buffer were brought to 1.5 M NDSB, efficient to prevent protein aggregation, and to 0.5 M GdmCl, at about 0.2–0.3 mg/mL final protein concentration. Thermograms normalized for protein concentration were analyzed for T_{max} (top of the transition) and ΔH_{cal} (area under the transition) using the MicroCal Origin software (version 7).

2.6. Dynamic light scattering

Dynamic light scattering data were recorded on a DynaPro NanoStar instrument (Wyatt Technology Corporation) operated in batch mode and fitted with a laser beam emitting at 658 nm with power autoattenuation. The scattering angle was 90° for the DLS avalanche photodiode. Samples were filtered on Whatman Anotop 10 inorganic membrane (0.02 μm cut off) and loaded into a 10 μL quartz microcuvette. Data were averaged from 20 acquisitions of the scattered light intensity during 5 s. Scattering data were analyzed using DYNAMICS v. 7.1.1.3 software (Wyatt Technology Corp.) that includes the DYNALS module for distribution analysis in photon correlation spectroscopy.

2.7. Circular dichroism spectroscopy

Circular dicroism (CD) spectra were recorded with a Jasco J-715 spectropolarimeter (Model PTC-348WI). The spectropolarimeter was calibrated with an aqueous solution of d-10-(+)-camphorsulfonic acid at 290 nm [33]. Molar ellipticity per mean residue, [θ] in $deg \cdot cm2 \cdot dmol^{-1}$, was calculated from the equation: $[\theta] = [\theta]_{obs} \cdot mrw \cdot (10 \cdot l \cdot C)^{-1}$, where $[\theta]_{obs}$ is the ellipticity measured in degrees, mrw is the mean residue molecular weight (111.6 Da), C is the protein concentration in g/mL and l is the optical path length of the cell in cm. A protein stock solution of each protein (0.5 mg/mL) in piperazine-N, N′-bis(ethanesulfonic acid) (PIPES buffer) 10 mM, pH 7.4, was diluted into buffer to achieve a normalized starting ellipticity of −13.0, using a final protein concentration of 0.2 mg/mL. CD spectra in the far-UV region were recorded from 190 nm to 250 nm in a 0.1 cm path length cell with a final protein concentration of 0.2 mg/mL. Near-UV CD spectra were recorded from 250 nm to 320 nm using about 2 mg/mL protein samples and 0.5 cm path length cells. CD spectra were recorded with a time constant of 4 s, a 2 nm bandwidth and a scan rate of 20 nm/min; the signal was averaged over at least three scans and baseline was corrected by subtracting a buffer spectrum.

2.8. Limited proteolysis

Limited proteolysis experiments were carried out by incubating SsMTAPII and its mutants with proteinase K. Enzymatic digestion was performed in 10 mM Tris–HCl pH 7.4, at 37 °C. The final mass ratio of substrate protein to protease was 67:1. At different incubation times the hydrolysis was stopped by the addition of phenylmethylsulfonyl fluoride (PMSF) (final concentration 250 μM) and the samples were assayed for MTA phosphorylase activity at 70 °C. The digested material (5 μg) was submitted to SDS-PAGE followed by staining with Coomassie brilliant blue R-250. For the amino acid sequence analysis, samples of the digested protein after SDS-PAGE, were electrophoretically blotted onto a polyvinylidene fluoride membrane utilizing a Bio-Rad Mini trans-blot transfer cell apparatus (Bio-Rad, Hercules, CA, USA). Transferred proteins were stained with Coomassie blue (0.1% in 50% methanol) for 5 min, destained in 50% methanol and 10% acetic acid solution for 30 min at room temperature and allowed to air dry. Stained protein bands were excised from the blot and their N-terminal sequences were determined.

3. Results and discussion

3.1. Design and general properties of SsMTAPII disulfide variants

Results from a detailed spectroscopic characterization of SsMTAPII and from thermal and GdmCl-induced unfolding/refolding experiments have demonstrated that disulfide bonds are crucial for the structural stability of the enzyme and that the denaturation of SsMTAPII is not a reversible equilibrium [34]. Nevertheless, both the chemical and thermal unfolding of the enzyme become reversible processes under reducing conditions, therefore suggesting that the loss of these covalent links weakens the tightly compact structure of the native protein and allows the reversible transition between the native and denatured states before modifications of protein covalent scaffold induced by high temperatures and chemical denaturants that cause the irreversible protein denaturation [34]. On the basis of these results it appears evident that, although the folding of a protein is a spontaneous in vivo process, the structural compactness of SsMTAPII and the presence of multiple disulfide bonds do not allow a reversible denaturation in vitro. This impairs the measurement of the parameters associated with protein thermodynamic stability that, instead, requires fully reversible protein unfolding.

In an attempt to make the heat-induced unfolding of SsMTAPII reversible, we have designed a variant in which all the seven cysteine residues of the enzyme are substituted by serine. The protocol for the synthesis of this mutant protein proceeded through the sequential insertion of single point mutations. This allowed to obtain all possible cysteine-lacking variants. Fig. 1 summarizes the cysteine/disulfide mapping of SsMTAPII variants. When compared to the *wild-type*, *mut1* lacks one disulfide bond (C200-C262); *mut2* lacks the CXC motif (C259-C261); *mut3* lacks both the disulfide bond C200-C262 and the CXC motif; *mut4* lacks two disulfide bonds (C200-C262 and C138-C205) and the CXC motif, and displays a second free cysteine (C138) in addition to the native C164; *mut5* shows only C164. Finally, *mut6* represents a SsMTAPII variant lacking all cysteine residues. The synthesis of all these mutant proteins provided the opportunity to assess the effect of each substitution on the conformational stability and flexibility of

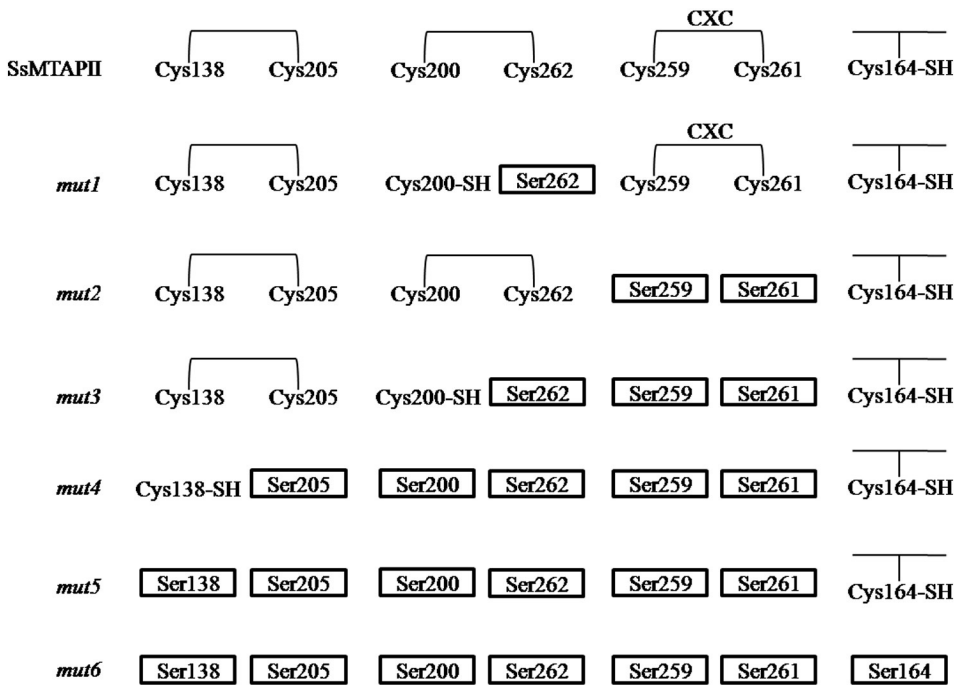

Fig. 1. Schematic representation of SsMTAPII disulfide variants. *mut1*, Cys262Ser; *mut2*, Cys259Ser:Cys261Ser; *mut3*, Cys259Ser:Cys261Ser:Cys262Ser; *mut4*, Cys259Ser:Cys261Ser:Cys262Ser:Cys200Ser:Cys205Ser; *mut5*, Cys259Ser:Cys261Ser:Cys262Ser:Cys200Ser:Cys205Ser:Cys138Ser; *mut6*, Cys259Ser:Cys261Ser:Cys262Ser:Cys200Ser:Cys205Ser:Cys138Ser:Cys164Ser.

SsMTAPII using kinetic and calorimetric characterizations and limited proteolysis.

The mutant proteins were expressed in native form in *E. coli* BL-21 cells. Large scale production was performed as described for *wild-type* SsMTAPII [24]. All proteins were found to be homogeneous on analysis on SDS-PAGE and showed, under either native or denaturing conditions, Mr values identical to the *wild-type*. Moreover, all SsMTAPII variants catalyzed efficiently MTA cleavage with specific activity values similar to the *wild-type* enzyme (Table 1).

3.2. Spectroscopic characterization of SsMTAPII disulfide variants

To analyze the effect of mutations on protein structure, a structural characterization of all enzyme variants was performed by circular dichroism (CD). As reported in Fig. 2A, the far-UV CD spectrum (190–250 nm) of *mut6*, i.e. the cysteine-free variant, appears almost indistinguishable from that of the *wild-type*, showing a similar positive band at 195 nm and a broad negative band centered at 222 nm, indicative of the presence of both α- and β-secondary structure elements. The same features have been observed for all SsMTAPII mutants (data not shown) indicating that the backbone conformation of the mutant proteins is similar to the *wild-type*. Moreover, the almost complete overlap of the near-UV CD spectra of the *wild-type* and of *mut6*, recorded in PIPES buffer 10 mM pH 7.4 at 25 °C (Fig. 2B) indicates that these proteins are isomorphous in their native states and that the complete removal of the disulfide bridges caused no significant change in their three-dimensional structure. These results, together with previous investigations [24], demonstrate that none of the disulfide bonds are critically involved in the correct SsMTAPII folding into the catalytically active conformation.

Table 1
Temperature dependence and thermostability of activity for SsMTAPII and its mutants.

	Optimum temperature (C°)	Temperature of half inactivation (C°)	Specific activity *units mg^{-1}
SsMTAPII	120	112	6.27
mut1	115	106	4.97
mut2	115	102	5.09
mut3	114	91	5.68
mut4	112	73	4.86
mut5	114	78	6.24
mut6	107	73	5.28

* Specific activity is expressed as μmol MTA cleaved per min per mg of protein at 70 °C. Errors are ±5% on activity and ±0.5 °C on temperature.

3.3. Kinetic characterization of the thermal properties of SsMTAPII disulfide variants

In order to compare the thermal features of the *wild-type* and of its variants in terms of thermostability, the temperature dependence of SsMTAPII activity was recorded for all variants. Subsequently, the effect of amino acid substitutions on enzyme thermostability was analyzed by short time kinetics of thermal denaturation. The plot of the residual activity after 5 min of preincubation as a function of temperature allowed to calculate the temperature for half inactivation (50% residual activity). As reported in Table 1, the mutations significantly reduce the optimal temperature for the catalytic activity, which decreases from 120 °C (*wild-type*) to 107 °C (*mut6*). Moreover, the elimination of the two disulfide bridges and the CXC motif causes a strong destabilization for the folded structure of the enzyme, as inferred from the temperature for half inactivation, which decreases from 112 °C (*wild-type*) to 73 °C (*mut6*).

3.4. Role of disulfide bridges in thermal stability assessed by differential scanning calorimetry

To elucidate the stabilization mechanisms of hyperthermophilic proteins, the stability in solution should be quantitatively determined and the energetic aspects stabilizing the proteins from a thermodynamic point of view should be elucidated. The measurement of parameters associated with protein thermodynamic stability requires fully reversible protein unfolding. Thermal unfolding of hyperthermophilic proteins, however, is often followed by rapid irreversible denaturation [35–37] as a consequence of formation of insoluble aggregates due to the sticky,

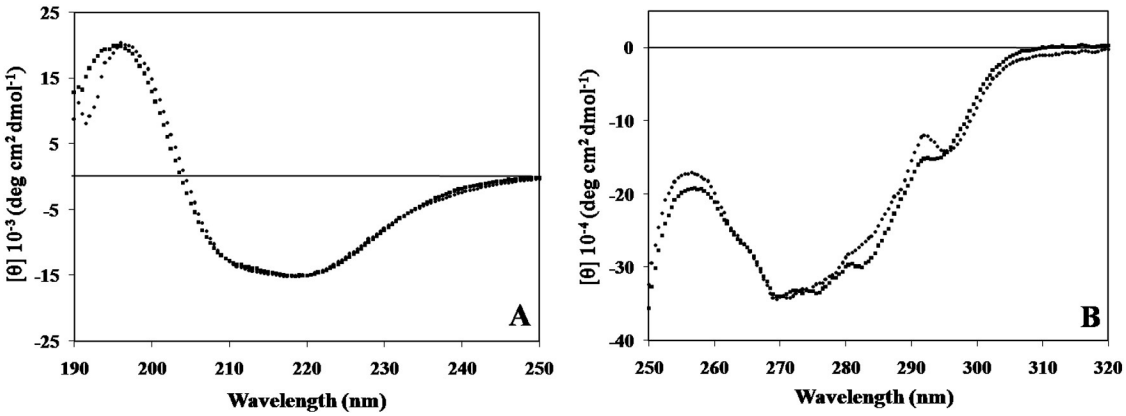

Fig. 2. Far-UV CD (A) and near-UV CD (B) spectra of SsMTAPII (■) and *mut6* (●) in PIPES buffer 10 mM, pH 7.4 at 25 °C. CD spectra in the far-UV region were recorded from 190 nm to 250 nm in a 0.1 cm path length cell with a final protein concentration of 0.2 mg/mL. Near-UV CD spectra were recorded from 250 nm to 320 nm using about 2 mg/mL protein samples and 0.5 cm path length cells.

hydrophobic nature of the exposed surfaces of the unfolded protein. Therefore, only few of such proteins, mainly small single-domain proteins, have been characterized in terms of their thermodynamic stability profiles [5].

Differential scanning calorimetry (DSC) allows a fine thermodynamic analysis of heat-induced unfolding of macromolecules and has significantly contributed to the elucidation of protein energetics [38]. Microcalorimetric studies of hyperthermophilic proteins are challenging as they unfold at the upper technical temperatures of DSC devices and are prone to massive aggregation at these high temperatures. In this study, we found suitable conditions to record reliable thermograms of SsMTAPII and of its mutants by using low protein concentrations (~0.2–0.3 mg mL^{-1} final protein concentration), fast scan rate (90 °C/h), and addition of a non-detergent sulfobetaine (1.5 M) [39] and of GdmCl (0.5 M) to prevent aggregation. As shown in the thermograms reported in Fig. 3, these experimental conditions delay and temporarily prevent protein aggregation in the microcalorimetric cell, allowing the recording of a stable post-transition baseline and the analysis of the heat-absorption peak. Nevertheless, thermal unfolding of SsMTAPII and all of its variants was found to be irreversible (after cooling and re-scan of the sample) presumably caused by the presence of aggregates. The irreversibility of the unfolding process has therefore limited the analysis to calorimetric parameters T_{max} (temperature at the top of the transition) and ΔH_{cal} (area under the transition, corresponding to all enthalpy-driven interactions broken during unfolding), that are reported in Table 2. Attempts to perform DSC under reducing conditions were unsuccessful as a result of the large heat background produced by reducing agents.

SsMTAPII displays a strong thermal stability as inferred from both the high T_{max} (111.6 °C) and calorimetric enthalpy (1110 kcal/mol) values. Disrupting the disulfide bond C200–C262 (leaving a free C200) in *mut1* destabilizes the enzyme: T_{max} decreases by 12 °C and ΔH_{cal} is reduced to about 66% of the *wild-type* value. However, removal in *mut2* of the CXC motif C259–C261 has an even more drastic destabilizing effect, leaving only 35% of SsMTAPII ΔH_{cal} value (393 kcal/mol). As both cysteines are only separated by a serine in the sequence, such a stabilization of SsMTAPII via a structural disulfide bond appear unrealistic. This rather suggests a functional role of this unusual disulfide in protein stability and further confirms previous results [26,27,34] demonstrating that the CXC motif in SsMTAPII can form a third disulfide bond that mimic PDI [21] to rescue the possible damage to the other two disulfide bridges.

Removal of both the above mentioned disulfide bridge C200–C262 and the CXC motif in *mut3* further decreases T_{max} (85.5–90.2 °C) without significant alteration of ΔH_{cal} with respect to *mut2* but mainly results in a biphasic unfolding transition, indicating the presence of two domains of distinct stability in this mutant enzyme.

Additional disruption of the disulfide bond C138–C205 (leaving a free C138) in *mut4*, decreases the stability of both domains observed in *mut3* that now appear completely resolved. Surprisingly, removal of C138 in *mut5* stabilizes this mutant with respect to *mut4* by increasing both the ΔH_{cal} (374 kcal/mol) and T_{max} (76.4–88.9 °C) values.

In the case of mutants *mut4* and *mut5*, which display two well resolved transitions, the possibility that the first transition could correspond to the hexamer dissociation was addressed by dynamic light scattering in the same buffer (data not shown). However, only an increase of the hydrodynamic radius was recorded in the temperature range of these first transitions, without evidence for the appearance of

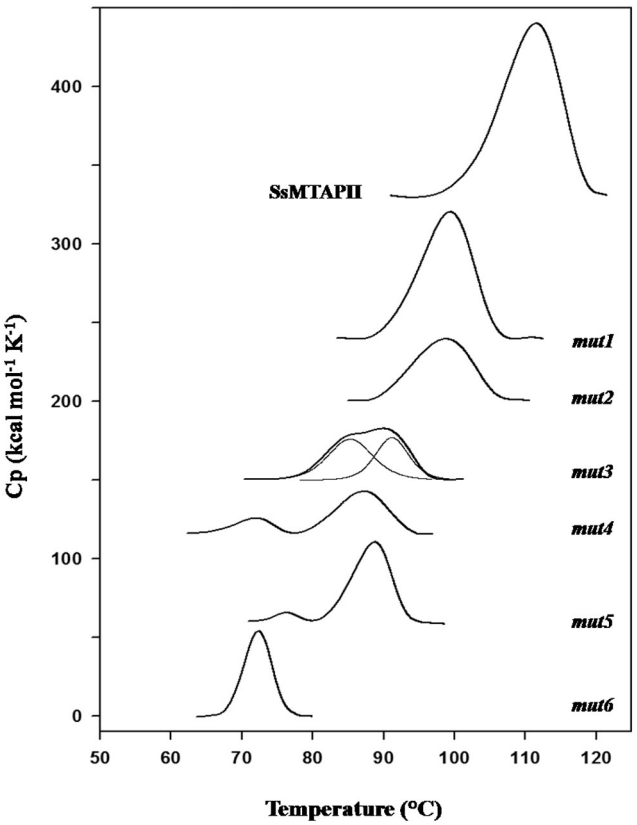

Fig. 3. Thermal unfolding of SsMTAPII and its mutants (0.2–0.3 mg/mL final protein concentration) recorded by differential scanning calorimetry. For clarity, the DSC traces have been displaced along the *Cp* axis, except for *mut6*. Deconvolution of *mut3* thermogram into two transitions is indicated by thin lines. Thermograms are recorded in 30 mM MOPS, pH 7.0, containing 1.5 M NDSB, and 0.5 M GdmCl.

Table 2
Thermodynamic parameters of heat-induced unfolding derived from differential scanning calorimetry.

Protein	ΔH_{cal} kcal mol^{-1}	T_{max} C°	$T1_{max}$ C°	$T2_{max}$ C°	ΔH_{cal} (T1) kcal mol^{-1}	ΔH_{cal} (T2) kcal mol^{-1}
SsMTAPII	1110	111.6				
mut1	729	99.5				
mut2	393	99.3				
mut3	386		85.5	90.2	217	169
mut4	292		71.8	87.4	64	228
mut5	374		76.4	88.9	25	349
mut6	262	72.3				

For biphasic thermograms, T_{max} and ΔH_{cal} (T1,T2) are given separately. Errors are ±10% on ΔH_{cal} and ±0.2 °C on T_{max}.

monomers. It can be concluded that the first DSC transition for both mutants reflects an unfolding event.

The observation that the presence of the free cysteine C164 makes *mut5* more stable than *mut4* suggests two different hypotheses. The first is that in *mut4* Cys138 probably performs unfavorable interactions with its immediate environment in the absence of its partner in the disulfide bond. The second is that in *mut5* the absence of disulfide bridges may allow C164 to form new stabilizing disulfide bond(s). Confirmation of the latter hypothesis has been provided by the results of SDS-PAGE of *mut5* carried out under reducing and nonreducing conditions. As shown in Fig. 4, when the experiment was carried out in the absence of 2-mercaptoethanol, a protein band at about 75 kDa (lane 4) appears in addition to that at 30 kDa (lane 3) observed under reducing conditions. These data are consistent with the presence of disulfide bond(s) probably localized intersubunit since the molecular mass observed in the absence of 2-mercaptoethanol corresponds approximately to the dimer of the enzyme. Different results are obtained when the *wild-type* is analyzed in the same experimental conditions. In fact, only one protein band at about 30 kDa was observed corresponding to the enzyme's monomer in which the cysteine residues might be either present in a reduced form (lane 2) or bound by

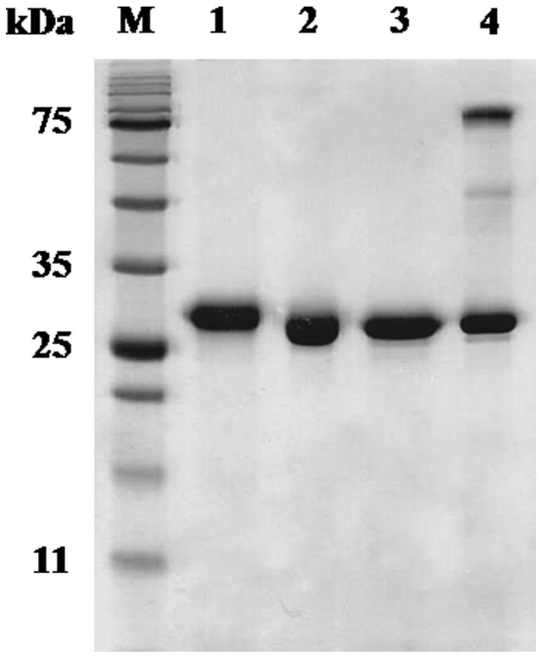

Fig. 4. SDS-PAGE pattern of SsMTAPII and *mut5*. The samples (5 μg) were subjected to SDS-PAGE under reducing and nonreducing conditions. M, molecular mass markers; lane 1, reduced SsMTAPII; lane 2, nonreduced SsMTAPII; lane 3, reduced *mut5*; lane 4, nonreduced *mut5*. Samples in lanes 1 and 3 were incubated for 40 min at 100 °C in 0.06 M Tris–HCl, pH 6.8, containing 2% SDS, 5% 2-mercaptoethanol, and 0.001% bromophenol blue prior to electrophoresis. Samples in lanes 2 and 4 were treated in the same experimental conditions without 2-mercaptoethanol.

intrachain disulfide bridges (lane 1) since this species appears after denaturation of the protein in the absence of reducing agents.

It is noteworthy that no intersubunit disulfide bonds have been evidenced in *mut3 and mut4* under the same experimental conditions, thus allowing to infer that the biphasic thermograms observed in these SsMTAPII variants should be ascribed to domains of distinct stability formed when the protein native disulfide bridges are eliminated in the absence of the CXC motif.

Finally, the removal in *mut6* of all cysteine residues, including the natively free C164 provides the least stable mutant of SsMTAPII (T_{max}, 72.3 °C; ΔH_{cal} 262 kcal/mol). It is worth mentioning that the low T_{max}, the weak ΔH_{cal} value and the uniformly unstable structure of *mut6* (leading to a perfectly symmetric transition) are strongly reminiscent of the microcalorimetric behavior of mesophilic proteins. Indeed, these proteins are usually stabilized by fewer weak interactions whose disruption strongly influences the whole molecular edifice promoting its cooperative unfolding. By contrast, the transition for thermophilic proteins is much less cooperative indicating the presence of structural blocks or units of distinct stability that unfold independently.

In conclusion, each disulfide bond contributes to varying degrees to the high Tm value of SsMTAPII. Moreover, the CXC motif also contributes to the enthalpic stabilization of SsMTAPII by about 65%, as inferred from the ΔH_{cal} values of mutants lacking this motif.

3.5. Role of disulfide bridges in conformational flexibility assessed by limited proteolysis

The protein native state prevailing under physiological conditions is not a single molecular species but is better described by an ensemble of statistically populated conformers. In this context, 'flexibility' refers to these fluctuating conformations of comparable energy that can be interconverted with a series of small changes. The larger the flexibility, the larger is the population of conformers and the lower is the energy barrier for interconversion between them [40].

On the basis of the three-dimensional structure of several proteins, it has been proposed that primary sites of proteolytic chain cleavage do not occur within chain segments having regular secondary structure (helices and sheets) but rather at the exposed loops [41]. A correlation between cleavage sites and sites of segmental mobility of the polypeptide chain has also been found [41]. Proteolytic enzymes, therefore, can be used to identify the sites of enhanced flexibility or of local unfolding propensity in the polypeptide chain [42].

We have previously demonstrated by limited proteolysis that SsMTAPII possesses only one proteolytic cleavage site localized in the C-terminal region and that the C-terminal peptide is necessary for the integrity of the active site [24]. It has been also demonstrated that the binding of MTA induces a conformational transition that protects the enzyme against protease inactivation [24]. It is interesting to note that the C-terminal region of SsMTAPII is highly flexible. In fact, as highlighted by the three-dimensional structure, the electron density of the C-terminus is relatively weak and the average B-factor of residues 262–270 is higher than the overall B-factor of the main chain [26].

To assess the native conformation of the SsMTAPII variants and to elucidate how disulfide bridges, CXC motif, and Cys164 affect the structural flexibility of the enzyme, each variant was subjected to limited proteolysis in comparison with the *wild-type*. The time course of proteolysis was investigated by measuring the residual activity after incubation with proteinase K at 37 °C, followed by SDS-PAGE of the digested material. As shown in Fig. 5A, the proteolytic pattern of the SsMTAPII variant lacking all cysteine residues (*mut6*) appears more complex than that of the *wild-type*. After 5 min incubation, the protease produced two major fragments among several proteolytic bands (lane 5). The first fragment, with a molecular mass slightly higher than that observed in *wild-type* (lane 2), probably marks the region where the unfolding process is initiated. The second fragment at about 18.5 kDa is rapidly

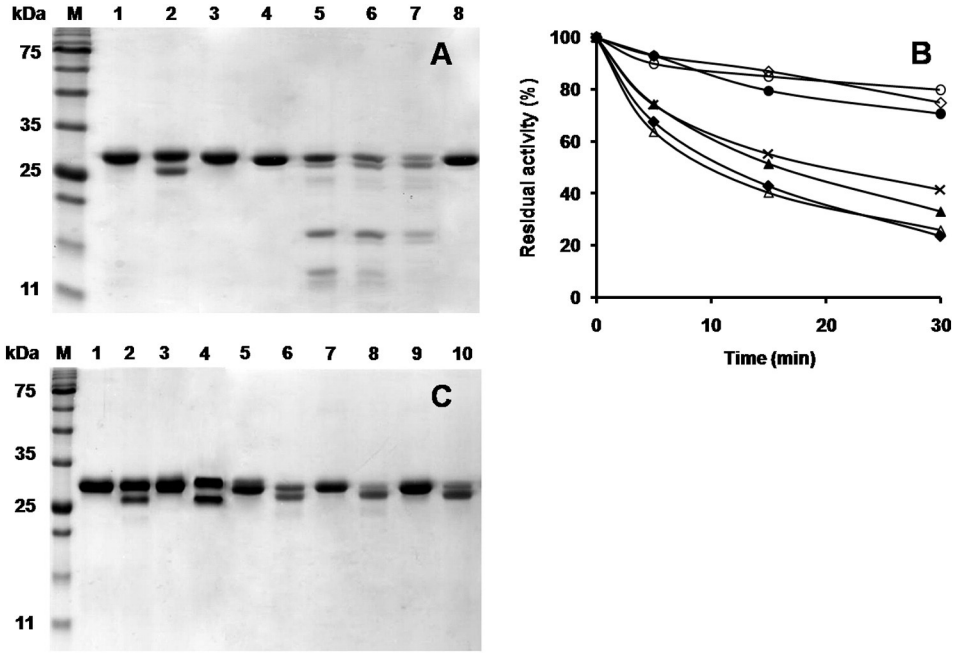

Fig. 5. Limited proteolysis of SsMTAPII and its mutant forms with proteinase K. A) SDS-PAGE, lane M, molecular mass markers; lane 1, SsMTAPII control; lane 2, SsMTAPII after 30-min incubation; lane 3, SsMTAPII after 30-min incubation in the presence of 5 mM MTA; lane 4, *mut6* control; lanes 5-7, *mut6* after 5-, 15-, and 30-min incubation; lane 8, *mut6* after 30-min incubation in the presence of 5 mM MTA. B) Time course for the hydrolysis of SsMTAPII and its mutants. SsMTAPII (○), *mut1* (◇), *mut2* (●), *mut3* (x), *mut4* (△), *mut5* (▲), *mut6* (♦). C) SDS-PAGE, lane M, molecular mass markers; lanes 1–10, *mut1*, *mut2*, *mut3*, *mut4*, *and mut5* (for each mutant, the control enzyme and the enzyme after 30-min incubation are shown). The concentration of protein used in the experiments is 0.003 mg/mL. The final mass ratio of SsMTAPII to protease was 67:1. Aliquots of enzymes at different incubation times at 37 °C with protease were taken from the reaction mixture and the hydrolysis was stopped (see Material and Methods). Samples were assayed for MTA phosphorylase activity at 70 °C, subjected to SDS-PAGE and gel stained with Coomassie brilliant Blue. Values given are the average from at least three experiments with standard errors (±5%).

degraded as the proteolysis proceeds and is likely a product of the proteolytic cleavage of the first fragment since, when analyzed by Edman degradation, the N-terminus is preserved. This also indicates that in *mut6*, the proteolytic cleavage site is localized in the C-terminal region as for the *wild-type*. After 30 min incubation, the first fragment (lane 7) becomes abundant, and the residual activity drops to 23.6% (Fig. 5B). By analogy with the *wild-type* (lane 3, Fig. 5A), when the experiments were carried out in the presence of the substrate MTA, *mut6* remained completely active and the proteolytic process did not occur (lane 8) indicating a MTA-induced conformational change. The results obtained indicate that, although the overall structure of *mut6* is quite similar to that of the *wild-type*, the loss of the two disulfide bonds, the CXC motif, and Cys164 causes an obvious disturbance of the native state resulting in a higher protease susceptibility and in a different proteolytic pattern.

It was also found that the relative contribution of each disulfide bond to enzyme flexibility depends on its location within the polypeptide chain. After 30 min of incubation with proteinase K, *mut1* and *mut2* (lanes 2 and 4 in Fig. 5C) showed a primary cleavage site and a proteolytic pattern similar to that of the *wild-type* (lane 2 in Fig. 5A) with comparable values of residual catalytic activity (Fig. 5B). These data indicate that the disulfide bond Cys200–Cys262 and the CXC motif exert only a moderate effect on the susceptibility of SsMTAPII to the proteolytic attack, in spite of the significant role played by these covalent links on enzyme thermostability (Table 2). It should be pointed out that Cys262 is positioned in a already very flexible region of the enzyme [26]. Similarly, the loop including Cys259 and Cys261 is located in a highly disordered area whose flexibility is crucial to allow the CXC motif to position very close to the two pairs of disulfide bond and to exert its stabilizing role through an oxidative folding mechanism [26,27]. It is therefore conceivable that the loss of CXC should affect the stability rather than the flexibility of SsMTAPII. The simultaneous elimination of Cys200–Cys262 disulfide bond and of CXC motif seems to play a synergistic effect on enzyme flexibility. In fact, after 30 min incubation the residual activity of *mut3* drops to 42%.

By contrast, the disulfide bond Cys138–Cys205 seems to contribute significantly in maintaining the native conformation of the enzyme. Indeed, after 30 min of proteolysis *mut4* appears very degraded by the protease; the primary proteolytic fragment becomes predominant (lane 8 in Fig. 5C) and the catalytic activity drops to 26%, a value similar to that observed in *mut6*. It is interesting to note that, as evidenced from the three-dimensional structure of SsMTAPII, Cys138 is located in helix α2, a zone of the enzyme involved either in the trimer–trimer interface or in the subunit–subunit interface within a trimer [26]. The loss of the disulfide bridge Cys138–Cys205 could therefore cause a deleterious disturbance of the compact structural organization of the enzyme thus causing ncreased protease susceptibility.

Finally, the limited proteolysis of *mut5*, where only C164 is present, gives insights on a possible stabilizing role of Cys164. As indicated by the time course of hydrolysis (Fig. 5B) and by the proteolytic pattern (lane 10 in Fig. 5C), *mut5* shows a protease susceptibility more similar to that of *mut3* (in which the disulfide bridge Cys138–Cys205 is still present) than that of *mut4*. It should be noted that Cys164 is located in the strand β9, near the protein surface but not directly exposed to solvent and not involved in the subunit–subunit interface within a trimer. [26]. This positioning makes Cys164 to far away from the cysteine residues, either in the same or in the neighboring monomers, to form disulfide bridges. This appears a quite strategic position at high temperatures. In fact, in the presence of disulfide bonds that tether the protein in the compact and rigid native state, the thermolabile amino acid residue Cys164 can be protected from the oxidation. By contrast, when disulfide bonds are damaged or destroyed because of environmental stress, the increased segmental mobility of the polypeptide chain allows Cys164 to perform novel stabilizing disulfide bond(s) with its partner from a neighboring monomer, as demonstrated above by SDS-PAGE under nonreducing conditions (Fig. 4).

In conclusion, the substantial decrease in the values of ΔH_{cal} (850 kcal/mol) and T_{max} (39 °C) observed by comparing *wild-type* and *mut6* demonstrates that all cysteine pairs, and especially the CXC motif C259–C261, as well as the free C164 significantly contribute to SsMTAP

thermal stability. Furthermore, as deletion of these cysteines does not alter the mutant activities, it can be concluded that they are essential elements involved in structural stability. Moreover, limited proteolysis experiments, in good agreement with the DSC characterization of SsMTAPII, highlight the peculiar stabilization strategy adopted by this hyperthermophilic protein in which two disulfide bonds, a PDI-like CXC motif and a free cysteine residue combine together to maintain the delicate balance between stability and flexibility required by the enzyme to remain stable and functionally active under extreme thermal environments.

Conflict of interest

All the authors declare no conflict of interest.

Transparency document

The Transparency document associated with this article can be found, in the online version.

Acknowledgements

The work was partially supported by the F.R.S-FNRS, Belgium (Fonds de la Recherche Fondamentale et Collective, contract numbers 2.4535.08, 2.4523.11 and U.N009.13) and by the Belgian program of Interuniversity Attraction Poles (iPros P7/44) initiated by the Federal Office for Scientific, Technical and Cultural Affaires.

References

[1] L. Sawle, K. Ghosh, How do thermophilic proteins and proteosomes withstand high temperature? Biophys. J. 101 (2011) 217–227.
[2] G. Feller, Protein stability and enzyme activity at extreme biological temperatures, J. Phys. Condens. Matter 22 (2010) 1–17.
[3] R. Sterner, W. Liebl, Thermophilic adaptation of proteins, Crit. Rev. Biochem. Mol. Biol. 36 (2001) 39–106.
[4] L.D. Unsworth, J. van der Oost, S. Koutsopoulos, Hyperthermophilic enzymes—stability, activity and implementation strategies for high temperature applications, FEBS J. 274 (2007) 4044–4056.
[5] K.A. Luke, C.L. Higgins, P. Wittung-Stafshede, Thermodynamic stability and folding of proteins from hyperthermophilic organisms, FEBS J. 274 (2007) 4023–4033.
[6] A. Razvi, J.M. Scholtz, Lessons in stability from thermophilic proteins, Protein Sci. 15 (2006) 1569–1578.
[7] S. Kumar, C.J. Tsai, R. Nussinov, Factors enhancing protein thermostability, Protein Eng. 13 (2000) 179–191.
[8] G. Vogt, S. Woel, P. Argos, Protein thermal stability, hydrogen bonds, and ion pair, J. Mol. Biol. 269 (1997) 631–643.
[9] L. Xiao, B. Honig, Electrostatic contributions to the stability of hyperthermophilic proteins, J. Mol. Biol. 289 (1999) 1435–1444.
[10] A. Szilágyi, P. Závodszky, Structural differences between mesophilic, moderately thermophilic and extremely thermophilic protein subunits: results of a comprehensive survey, Structure 8 (2000) 493–504.
[11] J. Okada, T. Okamoto, A. Mukaiyama, T. Tadokoro, D.J. You, H. Chon, Y. Koga, K. Takano, S. Kanaya, Evolution and thermodynamics of the slow unfolding of hyperstable monomeric proteins, BMC Evol. Biol. 10 (2010) 207–218.
[12] A. Mukayama, K. Takano, Slow unfolding of monomeric proteins from hyperthermophiles with reversible unfolding, Int. J. Mol. Sci. 10 (2009) 1369–1385.
[13] H.F. Gilbert, Molecular and cellular aspects of thiol–disulfide exchange, Adv. Enzymol. Relat. Areas Mol. Biol. 63 (1990) 69–172.
[14] P. Mallick, D.R. Boutz, D. Eisenberg, T.O. Yeates, Genomic evidence that the intracellular proteins of archaeal microbes contain disulfide bonds, Proc. Natl. Acad. Sci. U. S. A. 99 (2002) 9679–9684.
[15] G. Cacciapuoti, M. Porcelli, C. Bertoldo, M. De Rosa, V. Zappia, Purification and characterization of extremely thermophilic and thermostable 5′-methylthioadenosine phosphorylase from the archaeon *Sulfolobus solfataricus*. Purine nucleoside phosphorylase activity and evidence for intersubunit disulfide bonds, J. Biol. Chem. 269 (1994) 24762–24769.
[16] T.C. Appleby, I.I. Mathews, M. Porcelli, G. Cacciapuoti, S.E. Ealick, Three-dimensional structure of a hyperthermophilic 5′-deoxy-5′-methylthioadenosine phosphorylase from *Sulfolobus solfataricus*, J. Biol. Chem. 42 (2001) 39232–39242.
[17] J. Meyer, M.D. Clay, M.K. Johnson, A. Stubna, E. Münch, C. Higgins, P. Wittung-Stafshede, A hyperthermophilic plant-type [2Fe-2S] ferredoxin from *Aquifex aeolicus* is stabilized by a disulfide bond, Biochemistry 41 (2002) 3096–3108.
[18] G. Cacciapuoti, M.A. Moretti, S. Forte, A. Brio, L. Camardella, V. Zappia, M. Porcelli, Methylthioadenosine phosphorylase from the archaeon *Pyrococcus furiosus*.Mechanism of the reaction and assignment of disulfide bonds, Eur. J. Biochem. 271 (2004) 4834–4844.
[19] G. Cacciapuoti, S. Gorassini, M.F. Mazzeo, R.A. Siciliano, V. Carbone, V. Zappia, M. Porcelli, Biochemical and structural characterization of mammalian-like purine nucleoside phosphorylase from the archaeon *Pyrococcus furiosus*, FEBS J. 274 (2007) 2482–2495.
[20] E. Pedone, D. Limauro, S. Bartolucci, The machinery for oxidative protein folding in thermophiles, Antioxid. Redox Signal. 10 (2008) 157–169.
[21] B. Wilkinson, H.F. Gilbert, Protein disulfide isomerase, Biochim. Biophys. Acta 1699 (2004) 35–44.
[22] A. Bzowska, E. Kulikowska, D. Shugar, Purine nucleoside phosphorylases: properties, functions and clinical aspects, Pharmacol. Ther. 88 (2000) 349–425.
[23] M.J. Pugmire, S.E. Ealick, Structural analyses reveal two distinct families of nucleoside phosphorylases, Biochem. J. 361 (2002) 1–25.
[24] G. Cacciapuoti, S. Forte, M.A. Moretti, A. Brio, V. Zappia, M. Porcelli, A novel hyperthermostable 5′-deoxy-5′-methylthioadenosine phosphorylase from the archaeon *Sulfolobus solfataricus*, FEBS J. 272 (2005) 1886–1899.
[25] H.G. Williams-Ashman, J. Seidenfeld, P. Galletti, Trends in the biochemical pharmacology of 5′-deoxy-5′-methylthioadenosine, Biochem. Pharmacol. 31 (1982) 277–288.
[26] Y. Zhang, M. Porcelli, G. Cacciapuoti, S.E. Ealick, The crystal structure of 5′-deoxy-5′-methylthioadenosine phosphorylase II from *Sulfolobus solfataricus*, a thermophilic enzyme stabilized by intramolecular disulfide bonds, J. Mol. Biol. 357 (2006) 252–262.
[27] G. Cacciapuoti, I. Peluso, F. Fuccio, M. Porcelli, Purine nucleoside phosphorylases from hyperthermophilic *Archaea* require a CXC motif for stability and folding, FEBS J. 276 (2009) 5799–5805.
[28] F. Schlenk, D.J. Ehninger, Observations on the metabolism of 5′-methylthioadenosine, Arch. Biochem. Biophys. 106 (1964) 95–100.
[29] J. Sambrook, E.F. Fritsch, T. Maniatis, Molecular Cloning: A Laboratory Manual, 2nd edn Cold Spring Harbor Laboratory Press, Plainview, NY, 1989.
[30] K. Weber, J.R. Pringle, M. Osborn, Measurement of molecular weight by electrophoresis on SDS-acrylamide gel, Methods Enzymol. 26 (1972) 3–27.
[31] M.M. Bradford, A rapid and sensitive method for the quantitation of microgram quantities of protein utilizing the principle of protein-dye binding, Anal. Biochem. 72 (1976) 248–254.
[32] S.C. Gill, P.H. von Hippel, Calculation of protein extinction coefficients from amino acid sequence data, Anal. Biochem. 182 (1989) 319–326.
[33] S.Y. Venyaminov, J.T. Yang, Determination of Protein Secondary Structure, in: G.D. Fasman (Ed.), Circular dichroism and the conformational analysis of biomolecules, Plenum Press, New York 1996, pp. 69–107.
[34] G. Cacciapuoti, F. Fuccio, L. Petraccone, P. Del Vecchio, M. Porcelli, Role of disulfide bonds in conformational stability and folding of 5′-deoxy-5′-methylthioadenosine phosphorylase II from the hyperthermophilic archaeon *Sulfolobus solfataricus*, Biochim. Biophys. Acta 1824 (2012) 1136–1143.
[35] R.L. Baldwin, Energetics of protein folding, J. Mol. Biol. 371 (2007) (283-30).
[36] R. Jaenicke, G. Bohm, The stability of proteins in extreme environments, Curr. Opin. Struct. Biol. 8 (1998) 738–748.
[37] C. Moczygemba, J. Guidry, K.L. Jones, C.M. Gomes, M. Teixeira, P. Wittung-Stafshede, High stability of a ferredoxin from the hyperthermophilic archaeon *A. ambivalens*: involvement of electrostatic interactions and cofactors, Protein Sci. 10 (2001) 1539–1548.
[38] C.M. Johnson, Differential scanning calorimetry as a tool for protein folding and stabilitySee comment in PubMed Commons below Arch. Biochem. Biophys. 531 (2013) 100–109.
[39] S. D'Amico, G. Feller, A nondetergent sulfobetaine improves protein unfolding reversibility in microcalorimetric studies, Anal. Biochem. 385 (2009) 389–391.
[40] A.J. Baldwin, L.E. Kay, NMR spectroscopy brings invisible protein states into focus, Nat. Chem. Biol. 5 (2009) 808–814.
[41] A. Fontana, P. Polverino de Laureto, V. De Filippis, Molecular Aspects of Proteolysis of Globular Proteins, in: W.J.J. van den Tweel, A. Harder, R.M. Buitelaar (Eds.), Protein Stability and Stabilization, Elsevier Science Publishers, Amsterdam 1993, pp. 101–110.
[42] A. Fontana, P. Polverino de Laureto, B. Spolaore, E. Frare, P. Picotti, M. Zambonin, Probing protein structure by limited proteolysis, Acta Biochim. Pol. 51 (2004) 299–321.